ADVANCED FUNCTIONAL MATERIALS
www.afm-journal.de

Materials Views
www.MaterialsViews.com

$FeCl_3$-Based Few-Layer Graphene Intercalation Compounds: Single Linear Dispersion Electronic Band Structure and Strong Charge Transfer Doping

By *Da Zhan, Li Sun, Zhen Hua Ni,* Lei Liu, Xiao Feng Fan, Yingying Wang, Ting Yu, Yeng Ming Lam, Wei Huang,* and *Ze Xiang Shen**

Graphene has attracted much attention since its first discovery in 2004. Various approaches have been proposed to control its physical and electronic properties. Here, it is reported that graphene-based intercalation is an efficient method to modify the electronic properties of few-layer graphene (FLG). $FeCl_3$ intercalated FLGs are successfully prepared by the two-zone vapor transport method. This is the first report on full intercalation for graphene samples. The features of the Raman G peak of such FLG intercalation compounds (FLGIC) are in good agreement with their full intercalation structures. The FLGICs present single Lorentzian 2D peaks, similar to that of single-layer graphene, indicating the loss of electronic coupling between adjacent graphene layers. First principle calculations further reveal that the band structure of FLGIC is similar to single-layer graphene but with a strong doping effect due to the charge transfer from graphene to $FeCl_3$. The successful fabrication of FLGIC opens a new way to modify properties of FLG for fundamental studies and future applications.

1. Introduction

Graphene, a single layer of carbon atoms with hexagonal arrangement, has attracted enormous interest due to its excellent electric field-effect transport properties[1] and mass-less Dirac fermion-like charge carrier property.[2,3] Huge progress on graphene research has been achieved in recent years, including: the development of various methods for graphene fabrication;[1,4–7] the discovery of its unique electronic, thermal and mechanical properties;[1–3,8–11] and, the successful fabrication of prototype graphene-based devices.[12,13] However, many of the unique properties of graphene are accorded to single-layer graphene (SLG). It would be very desirable to modify few-layer graphene (FLG) samples so that they have similar properties to SLG.

Graphite intercalation compounds (GICs) are complex materials that are formed by insertion of atomic or molecular layers of different chemical species between graphite interlayer space.[14] The interlayer distance of graphite is dramatically increased due to presence of the intercalants, which strongly affects the electronic coupling between graphene layers, hence changing its properties. Moreover, due to the wide variation of intercalants, different physical properties can be achieved for GIC, including different electrical, thermal and magnetic characteristics.[14–16] Thus, graphene-based intercalation compounds would be an efficient method to modify the properties of FLG. Until now, there have been no experimental reports on few-layer graphene intercalation compounds (FLGIC) except the most recent report on Br_2 and I_2 intercalated FLG by Jung et al., where FLG is not fully intercalated according to their Raman spectra and the structural model.[17] In this work, fully intercalated $FeCl_3$-FLGIC have been successfully prepared and systematically investigated by Raman spectroscopy. Raman spectra of such FLGIC clearly reveal the single-layer graphene-like electronic structure and strong charge transfer-induced doping effect. First principle calculations are also carried out to confirm the experimental results.

2. Result and Discussion

2.1. Full Intercalation Structure of FLGIC Revealed by Raman G Peak Features

Stage number is a key factor for normal bulk-based GIC, where stage is defined as the number of graphene layers between the

[*] D. Zhan, L. Sun, Dr. L. Liu, Dr. X. F. Fan, Dr. Y. Y. Wang, Prof. T. Yu, Prof. Z. X. Shen
Division of Physics and Applied Physics
Nanyang Technological University
Singapore, 637371, Singapore
E-mail: zexiang@ntu.edu.sg
Prof. Z. H. Ni
Department of Physics
Southeast University
Nanjing, 211189, PR China
E-mail: zhni@seu.edu.cn
Prof. Y. M. Lam
School of Materials Science and Engineering
Nanyang Technological University
Singapore, 639798, Singapore
Prof. W. Huang
Institute of Advanced Materials
Nanjing University of Posts and Telecommunications
9 Wenyuan Road, Nanjing, 210046, PR China

DOI: 10.1002/adfm.201000641

© 2010 WILEY-VCH Verlag GmbH & Co. KGaA, Weinheim

adjacent intercalated layers.[18] Raman spectroscopy is an effective tool to confirm the intercalation stage of GIC by identifying the component and structure of G peak, an $E_{2g}^{(2)}$ in the plane vibrational mode of graphite. The frequency of the G peak in GIC is known to be affected by three factors: charge transfer, intercalate-coupling effect and change of lattice constant.[19,20] The degree of charge transfer usually dominate the frequency evolution.[19,21] For the case of $FeCl_3$-GIC, the position and shape of the graphene G peak can differ under different intercalation conditions. For example, the singlet G peak position can blue shifted to around 1612 cm^{-1} for stage 2 GIC, representing graphene layers flanked on one side by $FeCl_3$, or blue shifted to around 1626 cm^{-1} for stage 1 GIC, representing graphene layers flanked on both sides by $FeCl_3$.[22,23] Furthermore, singlet G peak splits into doublet structure for GIC with higher stage (stage >2) or mixed stages.[22,23] The position and intensity ratio of each component of doublet peaks can be used to confirm the exact situation.

$FeCl_3$-FLGIC was fabricated by the traditional two-zone method (see the Experimental Section). **Figure 1** presents the Raman spectra for graphenes (1 layer (1L) to 4 layers (4L)) after intercalation. For SLG, it is not possible to be intercalated. Instead, we find doping-induced stiffening and sharpening of the G peak (blue shifts from 1581 to 1604 cm^{-1}), which is quite normal for SLG after vacuum annealing and exposure to air.[24,25]

For 2L graphene intercalated by $FeCl_3$, the G peak position blue shifts to approximately 1612 cm^{-1} (G_1) from approximately

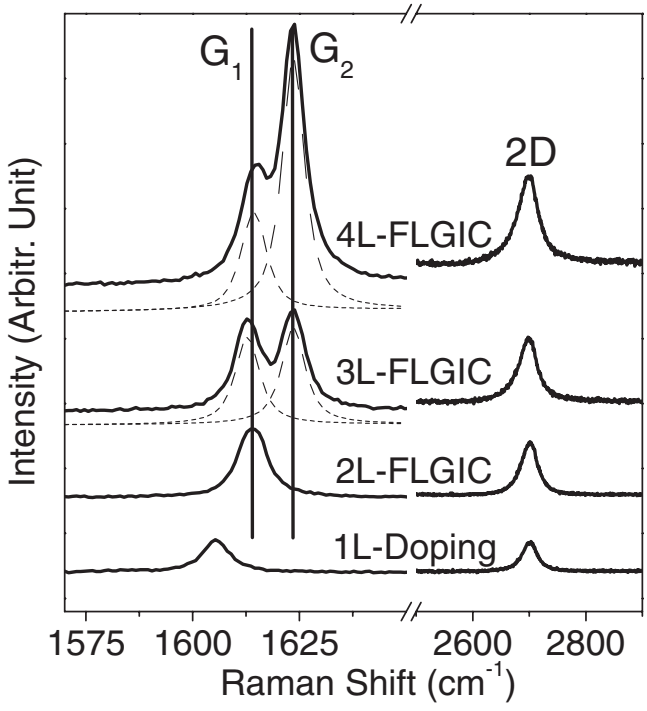

Figure 1. The Raman Spectrum of 1L doped graphene and 2L- to 4L-FLGIC. All the spectra were measured under same experimental conditions. The 2L-FLGIC shows a singlet G peak (G_1) at around 1612 cm^{-1}, while 3L- and 4L-FLGIC show doublet G peaks (G_1 and G_2 peaks located at approximately 1612 and 1623 cm^{-1}, respectively) with different intensity ratios. The G_1 and G_2 peaks are fitted with two dashed curves. Each spectrum shows single Lorentzian 2D peak and the intensity increases with the number of layers.

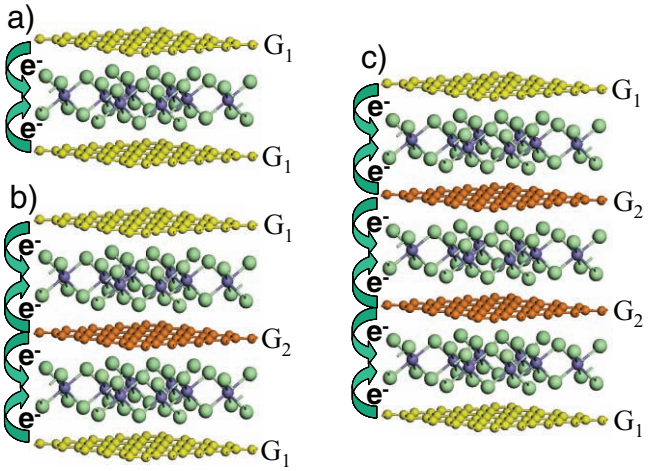

Figure 2. Schematic crystal structures of FLGIC : a) 2L-FLGIC; b) 3L-FLGIC; and, c) 4L-FLGIC. The model is constructed based on $FeCl_3$-GIC. [14,22,28] The graphene layers flanked on one/both side(s) by $FeCl_3$ layer(s) are denoted as yellow/orange. Cl atoms and Fe atoms are denoted as green and blue, respectively.

1580 cm^{-1} for pristine 2L graphene, which is similar to the previous reported G peak position of stage 2 bulk GIC.[22,23] Such a large blue shift (around 32 cm^{-1}) in G peak cannot be due to substrate and interface charge density doping,[26,27] which normally only introduce a shift of less than 10 cm^{-1}. The similar Raman spectra of 2L-FLGIC and stage 2 GIC can be explained by their similarity in structures. For 2L-FLGIC, both graphene layers are flanked on one side by $FeCl_3$ layer (**Figure 2a**), as for the structure of stage 2 GIC. Thus, it is reasonable that the G peak of 2L-FLGIC still presents one singlet peak and its position is similar to that of stage 2 bulk GIC.

For 3L and 4L graphene fully intercalated by $FeCl_3$, both present a doublet G band, with one peak located at around 1612 cm^{-1} (G_1) and the other at approximately 1623 cm^{-1} (G_2). Figure 2b and c show the schematic structures of 3L and 4L FLGIC, respectively; the top and bottom graphene layers (carbon atoms in yellow) are flanked on one side by $FeCl_3$ layers, and they contribute to the G_1 peak similar as in 2L-FLGIC; hence, the peak intensity of G_1 is almost same for 2L to 4L-FLGIC (Figure 1). The middle graphene layer(s) (carbon atoms in orange) is (are) flanked on both sides by $FeCl_3$ layers, which is similar to the case of stage 1 $FeCl_3$-based bulk GIC,[22,23] and they contribute to the more blue-shifted G_2 peak at around 1623 cm^{-1}. The integrated intensity ratio I_{G1}/I_{G2} is in the range 1.2–1.8 and 0.4–0.8 for 3L-FLGIC and 4L-FLGIC, respectively, which are close to ratio of 2 and 1 according to the schematic crystal structure illustrated in Figure 2b and 2c.

2.2. Strong Charge Transfer Chemical Doping

The stiffening of the $E_{2g}^{(2)}$ phonons (blue shift of G_1 and G_2 peaks) of the graphene layer for $FeCl_3$-FLGIC is mainly due to the charge transfer-induced doping effect,[17] where the graphene layer can be considered to be hole-doped since $FeCl_3$ is an acceptor-type intercalant.[20] The strong charge transfer

© 2010 WILEY-VCH Verlag GmbH & Co. KGaA, Weinheim

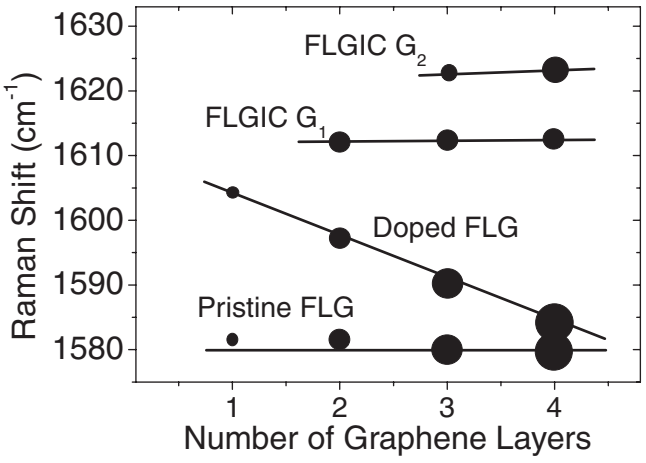

Figure 3. Comparison of the G-peak position of FLGIC, doped FLG and pristine FLG. The SLG after the intercalation process has a similar spectrum to doped SLG and they are overlapped. The intensity of the G peak is represented by the radius of the solid circles.

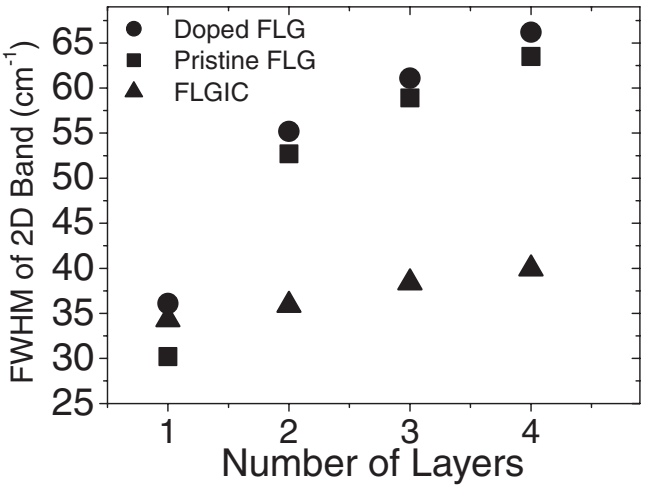

Figure 4. FWHM of the 2D peak of doped FLG (circles), pristine FLG (squares) and FLGIC (triangles). Note that the doping instead of intercalation for the 1L case.

effect induces a downshift of the Fermi surface of graphene and causes stiffening of the G peak due to the non-adiabatic removal of the Kohn anomaly at the Γ point.[29–31] The larger blue shift of the G_2 peak compare with the G_1 peak is because the inner graphene layers are affected on both sides by the $FeCl_3$ layers (G_2), while the outer layers are only affected on one side (G_1). In addition to stiffening effect of $E_{2g}^{(2)}$ phonons, the much smaller linewidths of G_1 (approximately 7 cm^{-1}) and G_2 (approximately 6 cm^{-1}) peaks compared to that of pristine graphene (around 15 cm^{-1}) are also observed, which is another indication of the strong doping effect on graphene.[29]

The G-peak positions of FLGIC samples versus the number of graphene layers is shown in **Figure 3**. For comparison, G-peak positions of pristine graphene samples as well as doped graphene samples are also included. The G peak position of pristine graphene is almost independent of the number of layers. For doped 1L graphene, obvious blue shifts were observed approximately from 1580 to 1605 cm^{-1}. The amount of blue shift is decreased with the increase of graphene layer number from 2L to 4L. On the other hand, for FLGIC, the phenomena are totally different. For 2L-FLGIC, the G peak blue shifts to 1612 cm^{-1}, and it splits into two peaks (G_1 and G_2) when the number of graphene layers increases to 3 or more. The G_1 peak intensity is almost constant in our experiments, while the G_2 peak intensity becomes stronger with the increase of the graphene layer number. The intensity of the peaks is represented by the size of the solid circles in Figure 3. The trend of the G_1 and G_2 intensity evolution from 2L- to 4L-FLGIC implies that, with increasing number of graphene layers, the G_2 peak will gradually dominate the doublet G band and finally it should present as a single peak, as for the stage 1 bulk-based GIC case (approximately 1626 cm^{-1}).[22,23]

2.3. Electronic Band Structure of FLGIC Probed by Raman 2D Peak

The 2D peak can be used as a fingerprint to identify layer numbers of pristine graphene, as it is originated from double resonance process and strongly dependent on the electronic band structure around K point at the Brillouin zone.[32] The 2D peak of fully intercalated FLGIC samples shows essential difference from that of pristine FLG in the following three aspects. i) Only one Lorentzian peak can be well fitted for all FLGIC samples (2L-to 4L-FLGIC), as shown in Figure 1; this is similar to the 2D peak of SLG[33] as well as mis-oriented graphene or folded graphene.[34] In contrast, the 2D peak of pristine 2L graphene can be fitted by four Lorentzian peaks and those of other FLG are fitted by many Lorentzian peaks.[32,33] ii) The linewidth of the 2D peak of FLGIC is much sharper than that of pristine FLG, as shown in **Figure 4**. For pristine and doped graphene, the linewidth dramatically broadens from 1L to a few layers. However, for FLGIC, the 2D linewidths are much sharper than FLG and they only show slight broadening with increasing number of layers. iii) The 2D peak integrated intensity of pristine FLG does not change with the increased number of graphene layers.[33] However, for FLGIC, 2D peak intensity increases with the number of layers (in Figure 1, all the spectra were measured under the same conditions).

The above differences of 2D peak properties between FLGIC and FLG are mainly for the following two reasons. i) The distance between adjacent graphene layers is enlarged from the original 3.4 Å to around 9.4 Å in the FLGIC samples.[22,23,28] Thus, adjacent graphene layers can only interact with each other through the intercalant layer, resulting in much weaker coupling, which in turn make the properties of FLGIC very similar to those of SLG, as indicated by sharp SLG-like 2D peaks. ii) Graphene and $FeCl_3$ are incommensurate in structure because the lattice constant of $FeCl_3$ and graphene are 6.06 and 2.46 Å,[14,22,28] respectively. Therefore, the coupling between graphene and $FeCl_3$ is very weak. As a result, the fully intercalated $FeCl_3$-FLGIC can be viewed as quasi-individual graphene layers superimposed together with a very weak coupling effect through the intercalant layers. The electronic properties of FLGIC behave like SLG with single dispersion near the Dirac point, resulting in single Lorentzian 2D peak with peak intensity increases with number of layers.

© 2010 WILEY-VCH Verlag GmbH & Co. KGaA, Weinheim

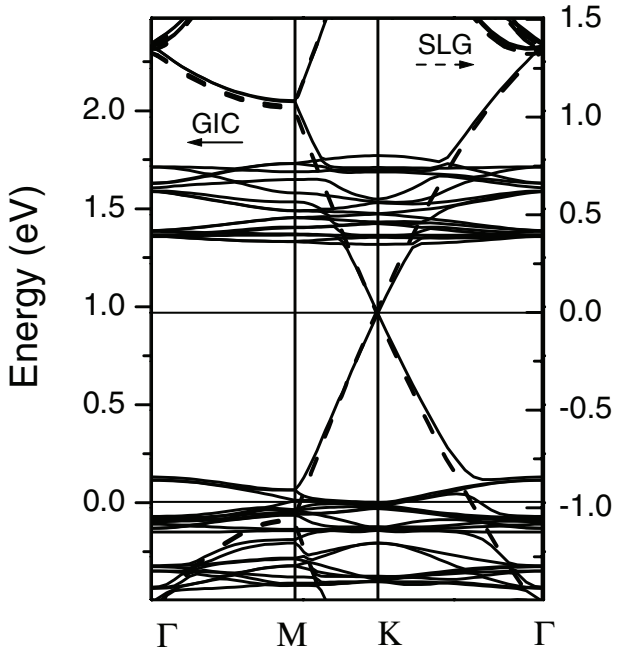

Figure 5. Electronic band structures of SLG (dashed lines) and $FeCl_3$-based stage 1 GIC (solid lines). The horizontal bands of GIC originate from the *d* orbital of iron. Except for those bands, the band structure of GIC and SLG are very similar. An obvious difference is that the Dirac point of SLG locates exactly at Fermi surface while that of GIC locates at around 1 eV, suggest that GIC is strongly hole-doped.

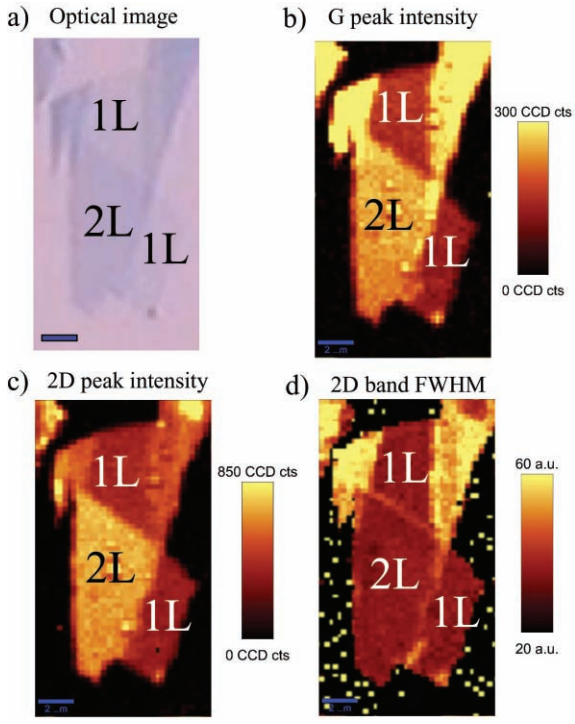

Figure 6. Raman images of 2L-FLGIC and 1L-graphene. a) Optical image of graphene samples before intercalation. b) Raman image of the G-peak intensity after intercalation. c) Raman image of the 2D peak intensity after intercalation. d) Raman image of the 2D peak FWHM (linewidth) after intercalation. The intensities of G and 2D peaks of 2L-FLGIC are much stronger than those of 1L graphene, while there is no noticeable difference in the 2D linewidth between 2L-FLGIC and 1L-graphene. The 2D linewidth of 2L-FLGIC region is uniform at around 35 cm^{-1}. The scale bar is 2 μm for all images.

2.4. Electronic Band Structure by First Principle Calculations

The calculated band structure of $FeCl_3$-based stage 1 GIC (solid lines) and SLG (dashed lines) are shown in **Figure 5**. The horizontal bands of GIC around 0 and 1.5 eV originate mostly from the *d* orbitals of iron. Except for those bands, the band structure of GIC is very similar to that of SLG, with single dispersion near the Dirac point. This agrees well with the Raman spectra of FLGIC, which show a single and sharp 2D peak. Considering the on-site Coulomb interaction of Fe^{3+} ions, the spin-dependent DFT calculation (LSDA+U) confirms the role of $FeCl_3$ insertion in FLG. While bringing little disturbance to the band of SLG, the main effect of the inserted $FeCl_3$ layers on SLG is shifting the Fermi level and transferring charges. The Fermi energy of FLGIC shifts to approximately 1.0 eV below the Dirac point, which indicates FLGIC is heavily hole-doped. This hole-doping effect induced by charge transfer from graphene to $FeCl_3$ explains the significant blueshift of G peak of FLGIC. The G_2 peak of FLGIC is at approximately 1623 cm^{-1}, which can be converted to the shift of Fermi level of 0.8–0.9 eV from the extrapolated gate-controlled doping result.[29] This again matches the calculated value of 1.0 eV quite well.

2.5. Homogenous Intercalation of $FeCl_3$ on FLGIC

Figure 6a shows an optical image of a graphene sample before the intercalation process. The 1L and 2L graphene were identified by Raman and contrast spectra before intercalation. Figure 6b and c, respectively, show Raman images of the G peak and 2D peak intensity after intercalation. The intensities of G and 2D peaks of 2L-FLGIC are much stronger than those of 1L graphene. However, the 2D peak linewidth does not show any noticeable difference between 1L graphene and 2L-FLGIC, as shown in Figure 6d. All the observed phenomena are consistent with the results in Figure 1 and 4. The uniform 2D linewidth across the whole 2L-FLGIC region indicates the homogenous intercalation of $FeCl_3$. $FeCl_3$-FLGIC samples are very stable in air ambient and the G and 2D Raman peaks have remain unchanged for 3 months to date. This result is similar to that for bulk-based $FeCl_3$-GIC.[35] In addition, no obvious D peak was observed for FLGIC indicating the good crystalline quality of graphene samples after intercalation.

Compared with the the Br_2- or I_2-based FLGIC reported recently,[17] FLGs can be fully intercalated by $FeCl_3$ more easily. This is not surprising as Br_2 usually creates stage 2 bulk GIC.[36] The observed complete quenching effect of 2D band in Br_2-FLGIC might be due to the commensurate structure between Br_2 and graphene layers, resulting in stronger interaction and modification of the electronic structure of graphene.[17,37] On the other hand, $FeCl_3$ is incommensurate with graphene and hence the interaction between $FeCl_3$ and graphene is minimum. The main effect of $FeCl_3$ intercalation is to: i) introduce

© 2010 WILEY-VCH Verlag GmbH & Co. KGaA, Weinheim

strong charge transfer doping; and, ii) increase the effective distance between the graphene layers; thus, the electronic structure of $FeCl_3$-based FLGIC becomes similar to that of SLG. Such effects could be further demonstrated by electrical transport measurements, where a significant shift of the neutral point (Dirac point) as well as characteristics of SLG (i.e., Berry's phase π)[38] should be present on FLGIC. Therefore, the electrical transport properties of FLGIC are presumably very interesting and deserving for further studies. The different effects of FLGIC using different intercalants suggest FLGIC offers a promising method to achieve desirable properties for FLG samples for both fundamental research and future applications.

3. Conclusions

In summary, ambient air-stable $FeCl_3$-FLGIC samples with a homogenous concentration of intercalant were successfully prepared. Our results show that FLG samples can be fully intercalated much more easily than bulk graphite, which normally takes around 6 d in a high concentration Cl_2 atmosphere.[39] Raman spectroscopy and imaging confirm that $FeCl_3$ is fully intercalated into FLG, while simultaneously introducing strong charge transfer chemical doping. FLGIC show single and sharp 2D peak, similar to that of single layer graphene, indicating the loss of electronic coupling between adjacent graphene layers. The observed phenomena agree very well with first principle calculations. FLGIC are quite promising materials not only because of the modification of the graphene electronic structure, but also due to the possible modification of electrical, thermal and magnetic properties through the choice of different intercalants, particularly Ca-FLGIC, which is expected to show superconductivity.[40]

4. Experimental Section

Fabrication of Pristine FLG, Doped FLG and FLGIC: Pristine graphene sheets were deposited by mechanical cleavage on silicon wafer covered by 300 nm thick SiO_2. The number of graphene layers (1 layer (1L) to 4 layers (4L)) was confirmed by Raman spectroscopy and their contrast spectra.[41,42] The two-zone vapor transport method was used for fabricating $FeCl_3$-FLGIC. The reaction took place inside a vessel constructed from a glass tube. The graphene samples and anhydrous $FeCl_3$ powder (approximately 0.03 g) were separated by around 6 cm. The tube was pumped to 10^{-2} torr and sealed. In our experiment, the two-zone method was processed using a single furnace instead of the traditional two-furnace technique. The temperature distribution in the furnace was measured by a thermocouple before the experiment. The reaction vessel was placed in an appropriate position in the furnace to achieve the desired two-zone temperatures (360 °C for graphene samples and 310 °C for anhydrous $FeCl_3$ powder). The heating rate was set at 10 °C min^{-1}, and the vessel was kept for 10 h at the set temperature. Finally the furnace was cooled at a rate of 10 °C min^{-1} to room temperature. The doped graphene was prepared by vacuum annealing of graphene at 900 °C for 10 min and then exposure to air at room temperature to obtain molecular (H_2O/O_2) doping.[24,25]

Raman Spectroscopy Measurements: Raman spectra were recorded by a WITEC CRM200 system with a spectral resolution of 1 cm^{-1}. The excitation laser was 532 nm (2.33 eV) and the laser power at sample was kept below 0.5 mW to avoid laser heating effect. A 100× objective lens with a numerical aperture of 0.95 was used. For Raman mapping measurement, a piezostage was used to move the sample with a step size of 250 nm and the Raman spectrum is recorded at every point in the scanned area.

Electronic Band Structure Calculation: The structure of $FeCl_3$-based stage 1 GIC modeled by Dresselhaus et al.[14,22,28] was simulated by density functional theoretical (DFT) calculations. A supercell with lattice constants $a = 12.12$ Å and $c = 9.370$ Å was constructed, where the layered $FeCl_3$ with 2×2 periods was taken as commensurate with the graphene of 5×5 unit cells, as shown in Figure 2. The DFT calculations based on the generalized gradient approximation (PBE-GGA)[43] were performed using the plane-wave basis VASP code.[44] The projector augmented wave (PAW) method is employed to describe the electron–ion interactions. A kinetic energy cutoff of 400 eV and k-points sampling with 0.05 $Å^{-1}$ separation in the Brillouin zone were used. The structure was optimized by a conjugate gradient algorithm with a force convergence criterion of 0.01 eV $Å^{-1}$.

Received: April 3, 2010
Revised: July 23, 2010
Published online: August 27, 2010

[1] K. S. Novoselov, A. K. Geim, S. V. Morozov, D. Jiang, Y. Zhang, S. V. Dubonos, I. V. Grigorieva, A. A. Firsov, *Science* **2004**, *306*, 666.
[2] K. S. Novoselov, A. K. Geim, S. V. Morozov, D. Jiang, M. I. Katsnelson, I. V. Grigorieva, S. V. Dubonos, A. A. Firsov, *Nature* **2005**, *438*, 197.
[3] Y. B. Zhang, Y. W. Tan, H. L. Stormer, P. Kim, *Nature* **2005**, *438*, 201.
[4] C. Berger, Z. M. Song, T. B. Li, X. B. Li, A. Y. Ogbazghi, R. Feng, Z. T. Dai, A. N. Marchenkov, E. H. Conrad, P. N. First, W. A. de Heer, *J. Phys. Chem., B* **2004**, *108*, 19912.
[5] S. Stankovich, D. A. Dikin, G. H. B. Dommett, K. M. Kohlhaas, E. J. Zimney, E. A. Stach, R. D. Piner, S. T. Nguyen, R. S. Ruoff, *Nature* **2006**, *442*, 282.
[6] A. Reina, X. T. Jia, J. Ho, D. Nezich, H. B. Son, V. Bulovic, M. S. Dresselhaus, J. Kong, *Nano Lett.* **2009**, *9*, 30.
[7] D. V. Kosynkin, A. L. Higginbotham, A. Sinitskii, J. R. Lomeda, A. Dimiev, B. K. Price, J. M. Tour, *Nature* **2009**, *458*, 872.
[8] S. Ghosh, I. Calizo, D. Teweldebrhan, E. P. Pokatilov, D. L. Nika, A. A. Balandin, W. Bao, F. Miao, C. N. Lau, *Appl. Phys. Lett.* **2008**, *92*, 151911.
[9] S. V. Morozov, K. S. Novoselov, M. I. Katsnelson, F. Schedin, D. C. Elias, J. A. Jaszczak, A. K. Geim, *Phys. Rev. Lett.* **2008**, *100*, 016602.
[10] J. H. Chen, C. Jang, S. D. Xiao, M. Ishigami, M. S. Fuhrer, *Nat. Nanotechnol.* **2008**, *3*, 206.
[11] A. A. Balandin, S. Ghosh, W. Z. Bao, I. Calizo, D. Teweldebrhan, F. Miao, C. N. Lau, *Nano Lett.* **2008**, *8*, 902.
[12] M. D. Stoller, S. J. Park, Y. W. Zhu, J. H. An, R. S. Ruoff, *Nano Lett.* **2008**, *8*, 3498.
[13] X. Wang, L. J. Zhi, K. Mullen, *Nano Lett.* **2008**, *8*, 323.
[14] M. S. Dresselhaus, G. Dresselhaus, *Adv. Phys.* **2002**, *51*, 1.
[15] T. E. Weller, M. Ellerby, S. S. Saxena, R. P. Smith, N. T. Skipper, *Nat. Phys.* **2005**, *1*, 39.
[16] N. Emery, C. Herold, M. d'Astuto, V. Garcia, C. Bellin, J. F. Mareche, P. Lagrange, G. Loupias, *Phys. Rev. Lett.* **2005**, *95*, 087003.
[17] N. Jung, N. Kim, S. Jockusch, N. J. Turro, P. Kim, L. Brus, *Nano Lett.* **2009**, *9*, 4133.
[18] P. C. Eklund, D. S. Smith, V. R. K. Murthy, S. Y. Leung, *Synth. Met.* **1980**, *2*, 99.
[19] C. T. Chan, K. M. Ho, W. A. Kamitakahara, *Phys. Rev. B: Condens. Matter Mater. Phys.* **1987**, *36*, 3499.
[20] T. Abe, M. Inaba, Z. Ogumi, Y. Yokota, Y. Mizutani, *Phys. Rev. B: Condens. Matter Mater. Phys.* **2000**, *61*, 11344.

© 2010 WILEY-VCH Verlag GmbH & Co. KGaA, Weinheim

[21] C. T. Chan, W. A. Kamitakahara, K. M. Ho, P. C. Eklund, *Phys. Rev. Lett.* **1987**, *58*, 1528.
[22] N. Caswell, S. A. Solin, *Solid State Commun.* **1978**, *27*, 961.
[23] C. Underhill, S. Y. Leung, G. Dresselhaus, M. S. Dresselhaus, *Solid State Commun.* **1979**, *29*, 769.
[24] L. Liu, S. M. Ryu, M. R. Tomasik, E. Stolyarova, N. Jung, M. S. Hybertsen, M. L. Steigerwald, L. E. Brus, G. W. Flynn, *Nano Lett.* **2008**, *8*, 1965.
[25] Z. H. Ni, H. M. Wang, Z. Q. Luo, Y. Y. Wang, T. Yu, Y. H. Wu, Z. X. Shen, *J. Raman Spectrosc.* **2010**, *41*, 479.
[26] I. Calizo, W. Z. Bao, F. Miao, C. N. Lau, A. A. Balandin, *Appl. Phys. Lett.* **2007**, *91*, 201904.
[27] Y. Y. Wang, Z. H. Ni, T. Yu, Z. X. Shen, H. M. Wang, Y. H. Wu, W. Chen, A. T. S. Wee, *J. Phys. Chem. C* **2008**, *112*, 10637.
[28] J. M. Cowley, J. A. Ibers, *Acta Crystallogr.* **1956**, *9*, 421.
[29] A. Das, S. Pisana, B. Chakraborty, S. Piscanec, S. K. Saha, U. V. Waghmare, K. S. Novoselov, H. R. Krishnamurthy, A. K. Geim, A. C. Ferrari, A. K. Sood, *Nat. Nanotechnol.* **2008**, *3*, 210.
[30] S. Pisana, M. Lazzeri, C. Casiraghi, K. S. Novoselov, A. K. Geim, A. C. Ferrari, F. Mauri, *Nat. Mater.* **2007**, *6*, 198.
[31] M. Lazzeri, F. Mauri, *Phys. Rev. Lett.* **2006**, *97*, 266407.
[32] L. M. Malard, M. A. Pimenta, G. Dresselhaus, M. S. Dresselhaus, *Phys. Rep.* **2009**, *473*, 51.
[33] A. C. Ferrari, J. C. Meyer, V. Scardaci, C. Casiraghi, M. Lazzeri, F. Mauri, S. Piscanec, D. Jiang, K. S. Novoselov, S. Roth, A. K. Geim, *Phys. Rev. Lett.* **2006**, *97*, 187401.
[34] Z. H. Ni, Y. Y. Wang, T. Yu, Y. M. You, Z. X. Shen, *Phys. Rev. B* **2008**, *77*, 235403.
[35] R. Schlogl, W. Jones, H. P. Boehm, *Synth. Met.* **1983**, *7*, 133.
[36] T. Sasa, Takahash. Y, T. Mukaibo, *Carbon* **1971**, *9*, 407.
[37] L. Liu, Z. X. Shen, *Appl. Phys. Lett.* **2009**, *95*, 252104.
[38] H. Schmidt, T. Ludtke, P. Barthold, E. McCann, V. I. Fal'ko, R. J. Haug, *Appl. Phys. Lett.* **2008**, *93*, 172108.
[39] S. R. Su, D. W. Oblas, *Carbon* **1987**, *25*, 391.
[40] I. I. Mazin, A. V. Balatsky, *arXiv:0803.3765v1*.
[41] Z. H. Ni, H. M. Wang, J. Kasim, H. M. Fan, T. Yu, Y. H. Wu, Y. P. Feng, Z. X. Shen, *Nano Lett.* **2007**, *7*, 2758.
[42] Y. Y. Wang, Z. H. Ni, Z. X. Shen, H. M. Wang, Y. H. Wu, *Appl. Phys. Lett.* **2008**, *92*, 043121.
[43] J. P. Perdew, K. Burke, Y. Wang, *Phys. Rev. B: Condens. Matter Mater. Phys.* **1996**, *54*, 16533.
[44] G. Kresse, J. Furthmuller, *Comput. Mater. Sci.* **1996**, *6*, 15.

© 2010 WILEY-VCH Verlag GmbH & Co. KGaA, Weinheim